ACI Concrete International, 2006, Vol. 28, No.1, pp.55-63.

Box Girder Bridge Deflections

Why is the initial trend deceptive?

BY VLADIMÍR KŘÍSTEK, ZDENĚK P. BAŽANT, MILOŠ ZICH, AND ALENA KOHOUTKOVÁ

The long-term deflection behavior of long-span prestressed concrete box girder bridges has often deceived engineers monitoring the deflections. Measuring small deflections over the first few years, the engineer is tempted to extrapolate and optimistically expect the deflections to remain small, only to be unpleasantly surprised when, after several years, the deflections suddenly accelerate. Without realistic calculations, one may even misinterpret the reasons for such a sudden acceleration of deflection and undertake inappropriate corrective actions that may induce excessive bending moments, overstressing the bridge, and possibly causing serious damage.

In these box girder bridges, the top slab typically has a uniform or nearly uniform thickness of about 200 mm (8 in.), while the bottom slab thickness can vary from about 200 mm (8 in.) at midspan to 1 m (3.3 ft) (or greater) at the supports. For a concrete slab, the rate of drying (and therefore the rate of shrinkage and drying creep) is roughly inversely proportional to the square of its thickness[1-6] and is further affected by differences in the temperature and relative humidity at its two surfaces. These differences are further magnified by solar heating on some exterior surfaces as well as by installation of an evaporation retarder (for example, an asphalt wearing course) on the top slab.

Although analysis methods for redundant structures with differential creep and shrinkage in the cross sections are well known,[7-9] creep and shrinkage effects on prestressed concrete box girder bridges are usually analyzed assuming the shrinkage strain and creep coefficients are uniform over the entire cross section of the box girder. The objective of this article is to show that this can result in severely incorrect predictions of long-term deflections and stress redistributions, especially when the initial deflections are extrapolated to later points in time. The predictions are incorrect even if the slab thickness is taken into account using classical prediction models, such as the one contained since 1972 in ACI 209R,[10] in which the effect of cross-section thickness on long-term creep and shrinkage is described by a strain multiplier rather than scaling of time.

The total calculated deflection of a prestressed box girder bridge represents a small difference between a downward deflection due to dead and live loads, and an upward deflection due to prestress. This small difference between two large, variable quantities is very sensitive to small errors in these deflections. A small change in one may cause a large percentage change in the total deflection. This is another reason why realistic prediction of differential creep and shrinkage is important.

RELEVANT CREEP AND SHRINKAGE PROPERTIES

To illustrate the effect of cross-section thickness on shrinkage over time, Fig. 1(a) shows shrinkage strains for various slab thicknesses predicted by a realistic creep and shrinkage prediction model— Model B3.[11,12] Although the ultimate shrinkage is about the same for all slab thicknesses, Fig. 1(a) clearly shows that thinner slabs shrink at a faster rate than thicker slabs.

Curves of creep strain per unit stress for sustained

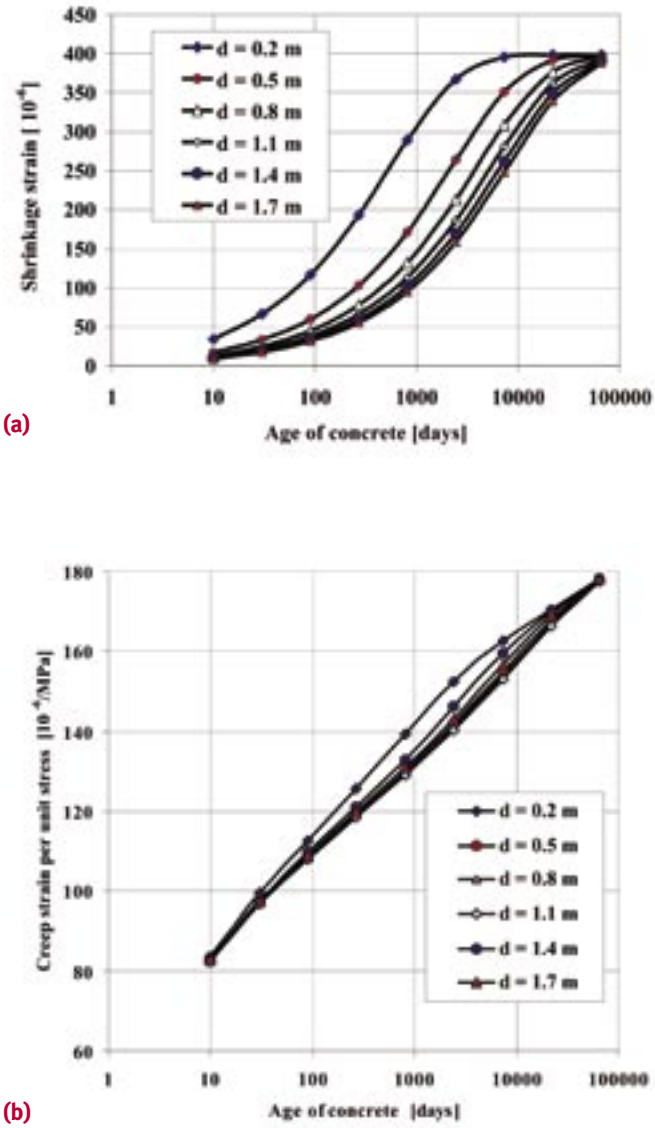

Fig. 1: (a) Shrinkage in flanges of different thicknesses; and (b) creep strain in flanges of different thicknesses

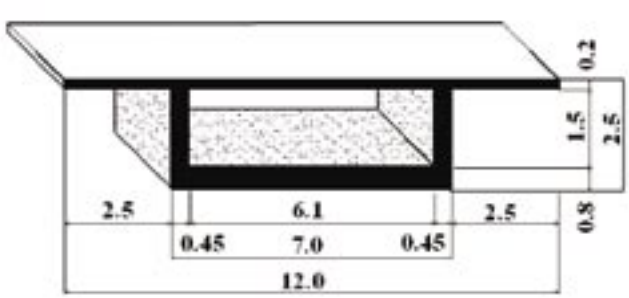

Fig. 2: Typical box girder segment with different top and bottom slab thicknesses (dimensions in meters, 1 m = 3.28 ft)

stress applied since the age of 7 days are shown in Fig.1(b) for various slab thicknesses. Despite a wide range of slab thicknesses [from 200 to 1700 mm (8 to 67 in.)], the creep strain per unit stress, unlike shrinkage, varies by less than 10%.

Nevertheless, creep may be important because even a small difference in creep strain among the individual parts of the cross section causes a coupling between the effects of bending moments and axial forces. An axial force applied at the centroid of the box cross section will produce not only axial displacement of the cross section but also an increase in rotation with time. Similarly, an applied bending moment will produce not only rotation but also increasing axial displacement at the centroid. Such moment-force coupling will change the lever arm and magnitude of the large prestressing force, which will, in turn, affect the curvature of the girder. The magnitude of these effects depends on the structural system and geometry (mainly on the differences in thickness) and also, of course, on the creep and shrinkage characteristics.

Traditional, simplified creep and shrinkage prediction models characterize only the overall behavior of the cross section and do not realistically capture the diffusion aspects of drying. The half-time of every diffusion process (the time to reach half of the final change) is roughly proportional to the square of the thickness.[1-4,6] Increasing the thickness of a slab from d to D does not reduce the ultimate shrinkage or drying creep by a thickness-dependent multiplier, as assumed in the existing ACI 209R recommendations.[10] Rather, the shrinkage gets delayed as if the passage of time was slowed down by a factor of d^2/D^2, which shifts the shrinkage curve a distance of $2 \log(D/d)$ to the right in the logarithmic plot.

Among the available models, Model B3[11,12] was chosen for this study. This model is scientifically justified by the known physical mechanisms of creep and shrinkage, optimally fits the relevant test data, agrees with all the required simple asymptotic trends, offers the widest choice of input parameters, and agrees with the theory of moisture diffusion including diffusion-based parameters for slab thickness and environmental humidity.[4] Although Model B3 takes almost half an hour to evaluate by hand, it is available, free of charge, on the Internet at **www.fsv.cvut.cz/~kristek** or **www.creep.fsv.cvut.cz/test/**.[13] After entering the relevant parameters, the user can instantly obtain the values of creep and shrinkage strain as well as the creep coefficient.

SEGMENT CURVATURE

The segment of a box girder shown in Fig. 2 with a bottom slab thickness ranging from 200 to 800 mm (8 to 31.5 in.) is used to demonstrate the effects of creep and shrinkage on the curvature and axial strains of a segment of a box girder over time. The following computational

results, based on Model B3 and the standard hypothesis of plane cross sections remaining plane, illuminate box girder behavior on several levels.

Shrinkage effects

With no external load applied to the drying box girder segment, incompatibility of the free shrinkage strains induced in the individual parts by drying produces a self-equilibrating distribution of axial stresses. Because these stresses produce creep, they must be taken into account. Although the plane cross sections assumption is not valid for a free-standing box girder segment, its use is justified because we are interested in the behavior of the box segment as an element within a long box girder.

Figure 3 shows curvature histories for various bottom slab thicknesses. If the bottom slab is thicker, its shrinkage lags compared to the top flange. Even if both the top and bottom slabs have the same thickness but different widths or surface conditions, a minor lag appears because of a difference in the volume-surface ratio. Consequently, a positive curvature initially develops that would cause upward deflections at the end of a cantilever. If the bottom slab is much thicker, the upward deflection can be large and continue for many years. A maximum upward deflection eventually occurs when shrinkage of the thin top slab nears completion and shrinkage of the thick bottom slab begins. After that, differential shrinkage causes negative curvature and downward deflections. If the bottom slab is very thick, significant downward deflection of the box girder occurs at a much later time than would commonly be expected.

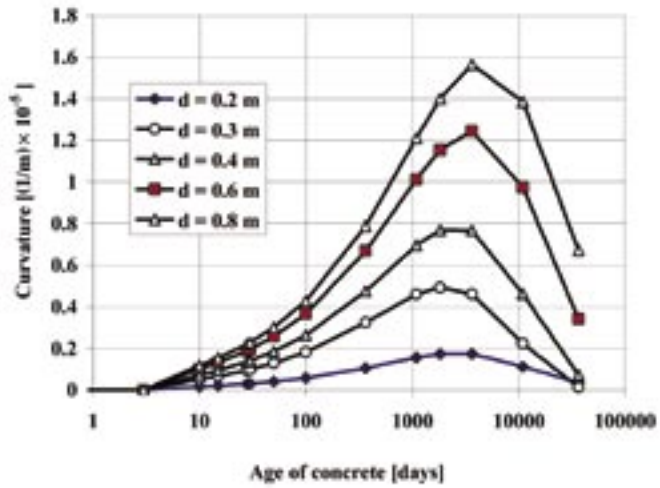

Fig. 3: Development of curvatures due to differences in top and bottom slab shrinkage rates

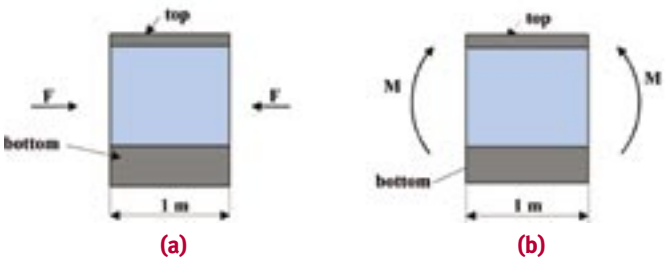

Fig. 4: Cross section subjected to: (a) axial force; and (b) bending moment

Drying with simultaneous axial force

An axial force producing a uniform compressive stress of 10 MPa (1450 psi) in the cross section, if acting alone, is shown in Fig. 4(a). Because it dries faster, the top slab initially creeps faster than the bottom slab, and the centroid of the transformed cross section corresponding to the effective modulus for creep moves downward. Therefore, an axial force applied at the original centroid produces an additional bending moment that slightly increases the initial upward curvature due to shrinkage. Similar to shrinkage, the effect of creep under axial force is eventually reversed. For a thick bottom slab, this occurs only after many years. The shift of the centroid of the transformed cross section also changes the lever arms of prestressing tendons. The combined effect, including drying, is shown in Fig. 5. Comparing Fig. 3 with Fig. 5 shows that there is only a slight increase in curvature due to the axial force.

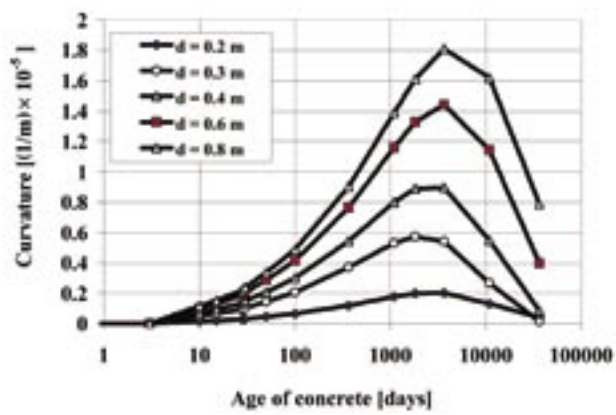

Fig. 5: Curvatures due to differential shrinkage with simultaneous axial force

Differential creep effects

To study differential creep separately, the box girder segment in Fig. 2 is subjected to a unit bending moment of magnitude M = 1 MN·m (740 kip·ft) at the age of 28 days, without simultaneous shrinkage (Fig. 4(b)). The creep strains in the top and bottom slabs evolve differently. The three curves plotted in Fig. 6 show how curvature varies with bottom slab thickness. For the upper curve,

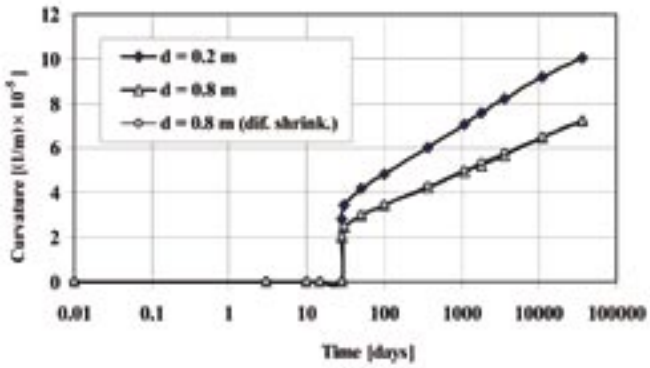

Fig. 6: Effect of differential creep on the development of curvatures

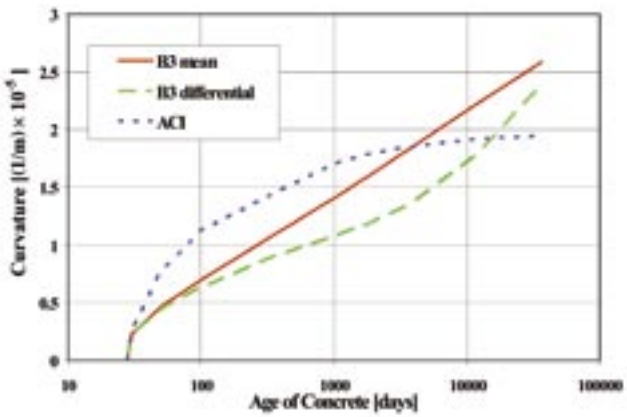

Fig. 7: Rate of element curvature variation according to different prediction models

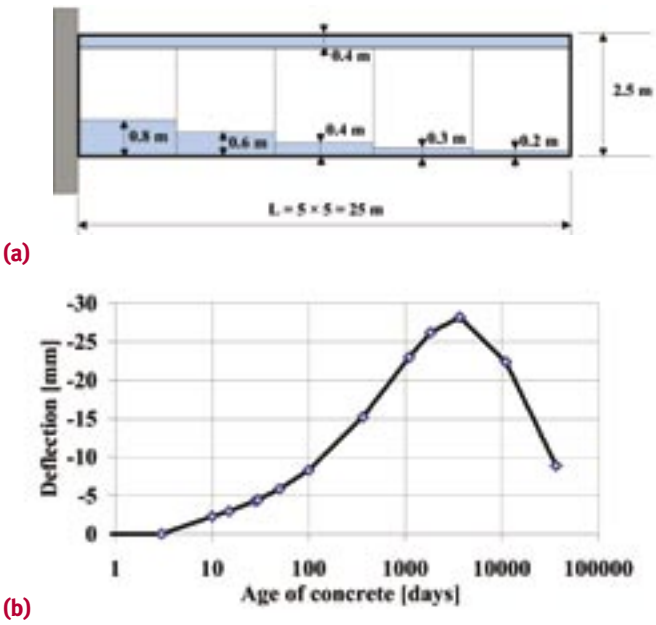

Fig. 8: (a) Cantilever with different bottom flange thicknesses; and (b) deflection of the free end of the cantilever due to differential shrinkage (1 m = 3.28 ft, 1 mm = 0.0394 in.)

both slabs have the same thickness of 200 mm (8 in.). The two nearly identical lower curves correspond to a bottom slab thickness of 800 mm (31.5 in.). One curve is obtained by neglecting the differences in drying rates of the top and bottom slabs by using the drying characteristics for the mean slab thickness, while the other includes these differences. These two curves differ by only about 1% because the differences in creep for slabs of different thicknesses are not very pronounced (Fig. 1(b)). Therefore, in contrast to differential shrinkage, the differential creep in slabs of different thicknesses does not play a significant role in curvature over time.

Drying with simultaneous bending moment

When a drying box girder segment is subjected to a bending moment (as in Fig. 4(b)), the differential shrinkage and differential creep are coupled. It is interesting to compare the curvature calculated considering only the mean humidity and the mean slab thickness (based on the overall volume-surface ratio of the cross section).

The comparison is shown in Fig. 7, which shows the curvature of a segment with an 800 mm (31.5 in.) bottom slab. Two of the curves in Fig. 7 are produced using Model B3. In one curve, the effects of thickness are neglected, whereas in the other, they are included. For comparison, a third curve, with a very steep initial rise, corresponds to the model from ACI 209R-92.[10] A long time-lag occurs between the curvature evolutions obtained when the differences in slab thicknesses are considered or neglected. In contrast to the usual simplified approach with one thickness, curvature (Fig. 7) begins to increase quickly several years after construction, or many years if the bottom slab is very thick.

BOX GIRDER DEFLECTION

Deflections are also influenced by the interaction of creep and shrinkage deformations in different box girder segments having varying bottom flange thicknesses. To examine this influence, a relatively short, 25-m-long (82 ft) box cantilever consisting of five segments with the bottom flange thicknesses shown in Fig. 8(a), was analyzed. End deflection of the cantilever due to differential shrinkage is plotted in Fig. 8(b). The upward deflection reaches its maximum of nearly 30 mm (1.2 in.) at 10 years, which illustrates the importance of differential shrinkage.

The simultaneous effects of differential shrinkage and a 1000 kN (225 kip) concentrated vertical force applied upward at the end of the cantilever is shown in Fig. 9. The upper curve indicates the deflections obtained when differential creep and shrinkage are taken into account, and the lower curve, when they are ignored. The large difference between the curves illustrates the importance of including differential creep and shrinkage.

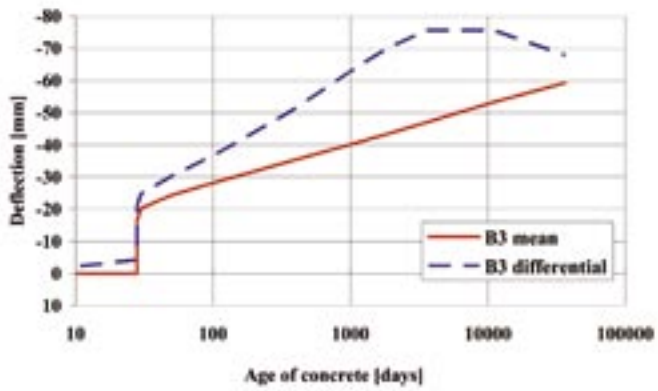

Fig. 9: Comparison of free-end deflections

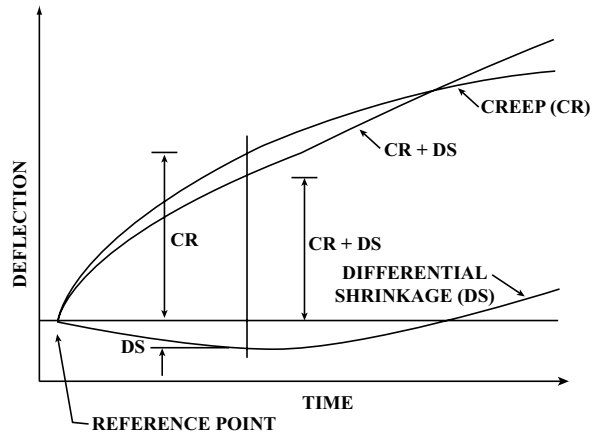

Fig. 10: Time-dependent contributions of creep and shrinkage to the total deflection

BOX GIRDER IN THE FINAL STRUCTURAL SYSTEM

Deflection of the cantilevers due to differential shrinkage occurs freely only until their ends are joined to create the final structural system. In practice, these joints are either hinged or moment-resisting.

For hinged joints, there is no restraint against continued rotation in the hinge and the vertical force that develops at the hinge is normally of little importance (unless the age difference between the two cantilevers is great). Therefore, bridge deflections due to differential shrinkage may continue to evolve almost freely, as in the original free cantilevers, and no significant secondary internal forces are induced in the structure after the cantilevers are joined.

For moment-resisting joints, a bending moment gradually develops in the joint as a result of creep because further relative rotations between the joined ends are prevented after the girder is made continuous. The symmetric part of the shrinkage will not produce any bending moments or deflections. As for the differential shrinkage, note that, in a clamped box girder of uniform cross section, it will induce no deflection changes after the cantilevers are joined. This is also approximately the case for an internal span of a long multispan continuous girder, provided that the girder is erected simultaneously in all spans. Long-span box girders erected by the cantilever construction method are typically tapered, having a variable cross section with different concrete ages in individual segments. But even for these complex situations, differential shrinkage causes only small and short-lived deflection variations in the final structural system with a moment-resisting joint. Generally, continuous box girders suffer much smaller deflections in the internal spans than girders with midspan hinges.

After installing a moment-resisting joint, significant additional redundant bending moments may nevertheless develop due to differential shrinkage. Their evolution can be quite complex, possibly changing from negative to positive values. The magnitude of these moments is roughly proportional to the girder stiffness. Thus, stiff cross sections near the support may produce bending moments that are quite high for the light cross sections near the midspan, resulting in significant additional stresses in the midspan region. Therefore, if differential shrinkage is ignored, the calculated stresses will be fictitious.

COMPARISONS TO FIELD MEASUREMENTS

As shown in Fig. 10 by the curve labelled CR+DS, drying shrinkage of the thinner top slab initially offsets downward deflections. However, once the thinner top slab has dried out and stopped shrinking, the slower shrinkage of the thicker bottom slab increases, causing large downward deflections. This can create serious problems for serviceability, durability, and long-time reliability of such bridges.

A survey of many bridges[14] monitored in various countries showed that all of them have experienced similar deflection histories. This observation strengthens the present message that the problems have one common systematic cause and do not result from local conditions, such as the kind of aggregate, cement type, climatic conditions, or shoddy labor. This survey includes 27 monitored bridges built by the cantilever method from 1955 to 1993. The bridges in the survey include 12 with hinges at midspan and 11 that are continuous; 22 cast-in-place bridges, and five assembled from precast segments; spans ranging from 100 to 140 m (330 to 460 ft); and observed deflections ranging from 120 to 200 mm (4.7 to 8 in.).

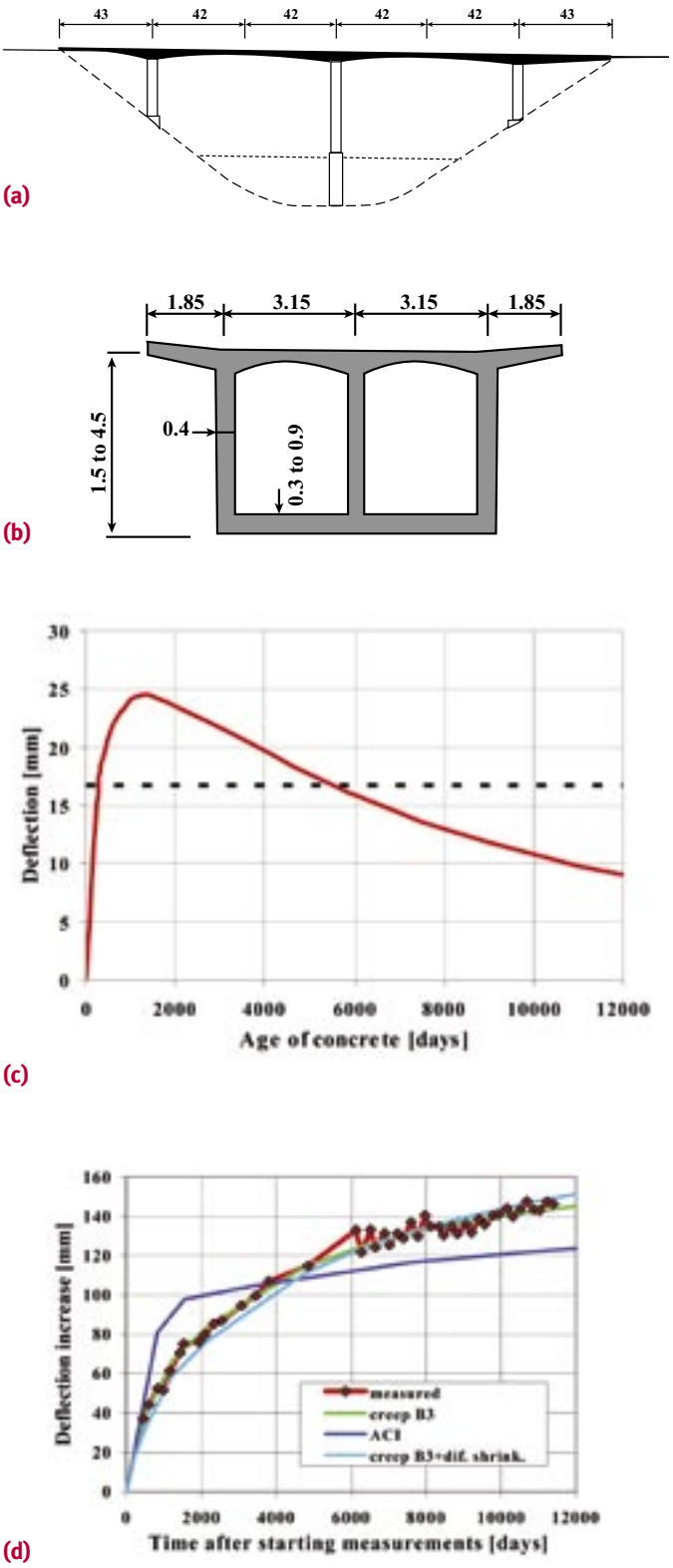

Fig. 11: Zvíkov Bridge over the Vltava River, built in 1962: (a) elevation; (b) cross section; (c) deflection component due to differential shrinkage; and (d) deflections measured or predicted by various models (all dimensions in meters, 1 m = 3.28 ft, 1 mm = 0.0394 in.)

The deflections of the cast-in-place bridges have continued to increase for very long periods and the slopes of the deflection curves are not leveling off, even after 30 years. On the other hand, the deflections of the precast segmental bridges have generally been smaller and have already stabilized, as predicted in design. The difference, compared to the cast-in-place bridges, may have several causes—the necessary compression reserve in the joints of segments naturally requires a higher level of prestress; the spans are generally shorter and thus the depth differences between cross sections above supports and at midspan are less; and the age of concrete at prestress application is generally much higher.

One bridge from this survey, the Zvíkov Bridge over the Vltava River, was built in 1962 in Southern Bohemia, Czech Republic, with hinges at midspan (Fig. 11(a) and (b)). As depicted in Fig.11(d), the midspan deflection reached about 140 mm (5.5 in.) after 30 years. In 1992, the bridge was repaired by installing moment-resistant joints that changed the structural system to a continuous frame.

Because short-term measurements and complete information on the precise concrete composition, strength, curing, and applied prestress are lacking, some estimates had to be made to carry out the analysis. The calculated deflections are shown in Fig. 11(d) for three analyses: 1) differential creep and shrinkage are ignored, with Model B3 used only for the mean cross-section characteristics; 2) differential creep and shrinkage included, with Model B3 used only for the mean cross-section characteristics; and 3) the ACI 209R-92 model is used (note that these three curves represent only the deflection increase after the start of monitoring).

The maximum upward deflection due to differential shrinkage and differential creep, which is nearly 25 mm (1 in.), was reached when the concrete was 1400 days old (Fig.11(c)). To obtain the deflection increase after monitoring was started, the diagram of the total deflections due to the differential shrinkage is shifted (as shown in Fig.11(c) by a thick horizontal dashed line). This shifted diagram is used as a component of the corresponding curve in Fig. 11(d).

A similar analysis was performed for the Lutrive Bridge, built in 1973 in Switzerland, which also had midspan hinges (Fig. 12(a) and (b)). The midspan deflections gradually increased to over 150 mm (5.9 in.) after 15 years, as depicted in Fig.12(d). The calculated deflections at midspan hinge due to differential shrinkage are plotted in Fig. 12(c). The maximum upward deflection was about 22 mm (0.87 in.) after 1300 days (the thick horizontal reference line corresponds to the start of deflection monitoring).

A comparison of the calculated and measured deflections is shown in Fig. 12(d), and it confirms the three main points of our preceding observations (Fig. 10): 1) the measured

deflections agree well with the calculations, taking into account differential shrinkage according to Model B3 (see Fig. 12(d)); 2) the time lag is captured in contrast to the calculations based on the mean cross-section behavior; and 3) the curve corresponding to the ACI 209R-92 model exhibits an excessively steep initial deflection curve and grossly underestimates long-term deflections.

CONCLUSIONS

Prestressed box girder bridges typically exhibit small deflections during the first years of service and then continue to deflect excessively. The cause is primarily a large difference in shrinkage between the top and bottom slabs of the box cross section and, to a small degree, a difference in drying creep. This difference is explained by a large difference between the top and bottom slab thicknesses and the proportionality of drying and shrinkage rates to the square of the thickness.

To predict long-term deflections correctly, the diffusion nature of drying must be realistically reflected in the creep and shrinkage prediction model.

An increase in slab thickness causes drying and shrinkage creep to be delayed, but not reduced by a multiplier. The delay should be proportional to the square of the thickness ratio.[1-3,6,11,12] Also, the shape of the drying and shrinkage creep curves in the model must not contradict diffusion theory, which means the initial shrinkage should evolve as a square root of drying time, and the final value should be approached exponentially.[4,11,12] Extensive monitoring on many bridges confirms these observations.

Other items not addressed in this article may also need to be considered. If high-strength concrete is used, autogeneous shrinkage must also be included in the analysis. Another point to emphasize is that, for greater reliability, it would be preferable to calculate not the mean deflection, based on the mean properties of concrete, but a 5% probability cutoff. This can be done by repeating the analysis for about ten different randomized samples of input parameters.

Acknowledgments

The authors are grateful for partial support obtained from the Infrastructure Technology Institute of Northwestern University (NU) under Grant No. 0740-350-A497, from the U.S. National Science Foundation under Grant No. CMS-0301145 to NU, from the Grant Agency of the Czech Republic under Grant No. 103/06/0674, and from the CIDEAS Research Center under Project No. 1M680470001. The first author appreciates his former appointment as Visiting Scholar at NU. Further thanks are due to J. Navrátil, Associate Professor at the Technical University of Brno (and former Visiting Scholar at NU), for making available his computer program TDA and for offering valuable comments, and to J.L. Vítek, Professor at CTU, Prague (and former Visiting Scholar at NU) for providing valuable technical information.

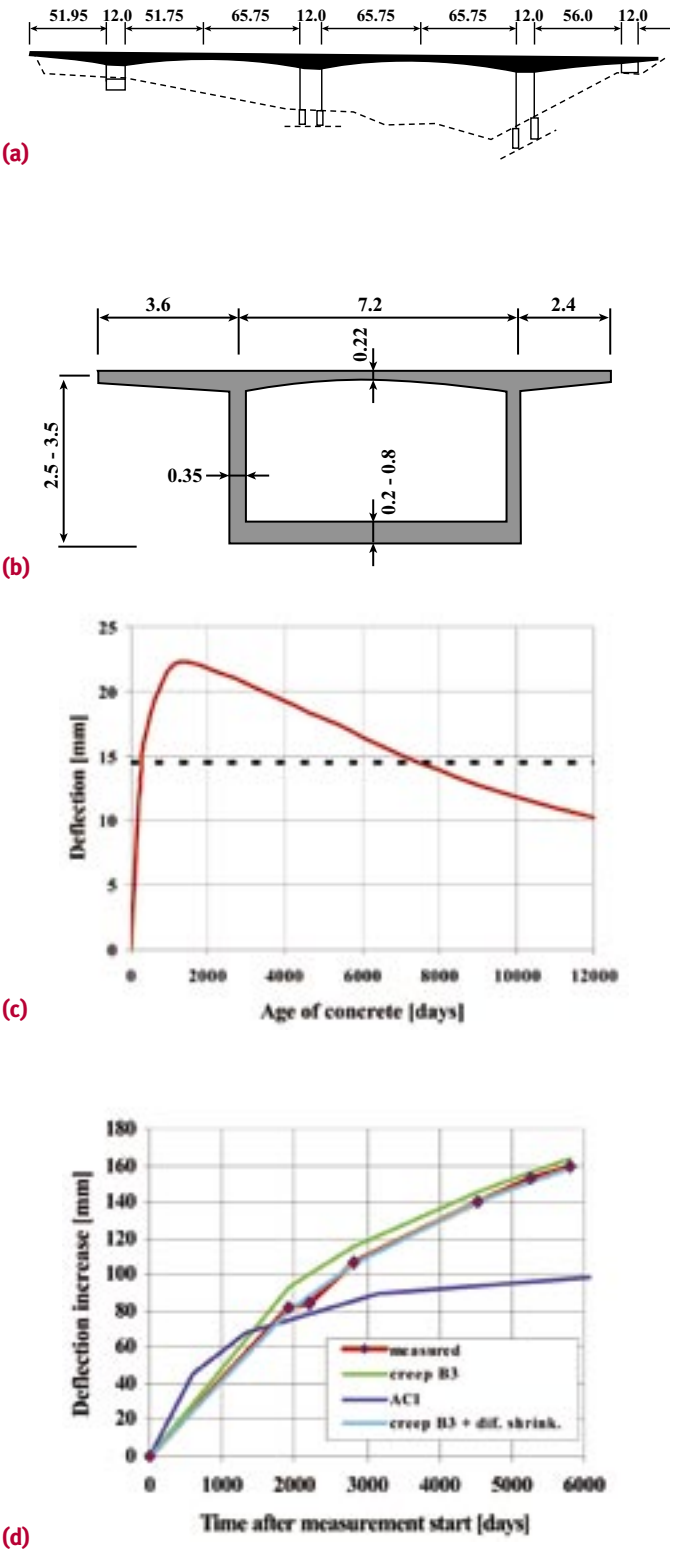

Fig. 12: The Lutrive Bridge: (a) elevation; (b) cross section; (c) deflection component due to differential shrinkage; and (d) deflections measured or predicted by various models (all dimensions in meters, 1 m = 3.28 ft, 1 mm = 0.0394 in.)

SIMPLE ILLUSTRATIVE EXAMPLE

It's instructive to give a simplified example amenable to short equations that anyone can check by hand calculation. Consider a cantilever of length L, drying in a constant environment, and consisting of an ideal box beam (with massless webs) and two flanges of different thicknesses d_1 and d_2, uniform over the individual segment lengths (Fig. A) but small enough for the moment of inertia of each flange cross section to be negligible. According to Model B3, the shrinkage strains in the top and bottom flanges at drying duration t are

$$\varepsilon_1 = \varepsilon_\infty \tanh\sqrt{t/\tau_1} \text{ and}$$
$$\varepsilon_2 = \varepsilon_\infty \tanh\sqrt{t/\tau_2}\text{, respectively,} \quad (1)$$

where ε_∞ is a constant, and τ_1 and τ_2 are the drying half-times of the flanges. According to diffusion theory,

$$\tau_1 = Cd_1^2 \text{ and } \tau_2 = Cd_2^2 \quad (2)$$

where C is a constant. The shrinkage produces positive curvature of a segment

$$k = (\varepsilon_1 - \varepsilon_2)/H_i \quad (3)$$

in which H_i is the box depth (Fig. A). The contribution of the i-th segment to deflection of the cantilever end due to differential shrinkage is

$$\Delta\delta_i = k_i s_i x_i \quad (4)$$

in which s_i is the length of the i-th segment, and x_i is the distance of its center from the cantilever free end (i = 1,2,…N). Thus, the deflection of the cantilever end due to differential shrinkage can be obtained as a sum of the contributions of individual segments;

$$\delta = \sum_{i=1}^{N} k_i s_i x_i \quad (5)$$

Considering the special case of uniform thicknesses of flanges d_1 and d_2 over the span length L, the deflection at the end of cantilever (positive if upward) can be approximated as

$$\delta = L^2 k/2 = \left(L^2/2H\right)\varepsilon_\infty\left[\tanh\sqrt{t/Cd_1^2} - \tanh\sqrt{t/Cd_2^2}\right] \quad (6)$$

Because, for a large bridge, d_2^2/d_1^2 may be as large as 30, it is clear that the first term in the bracket reaches its final value of 1 well before the second term becomes significant. After that, the second (negative) term grows in magnitude, causing the upward shrinkage deflection to decrease. This deflection history due to differential shrinkage is, of course, superposed on the creep deflection history.

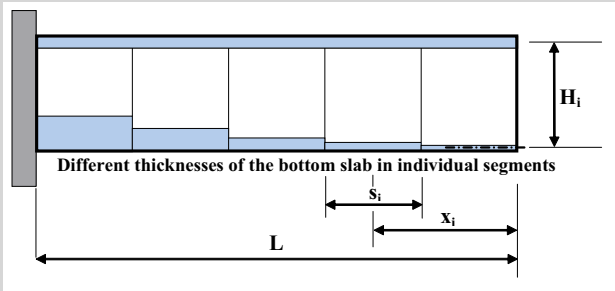

Fig. A: Simple illustrative example of a cantilever with a varying bottom flange thickness

References

1. Bažant, Z.P., and Najjar, L.J., "Nonlinear Water Diffusion in Nonsaturated Concrete," *Materials and Structures* (RILEM, Paris), V. 5, 1972, pp. 3-20 (reprinted in *Fifty Years of Evolution of Science and Technology of Building Materials and Structures*, F.H. Wittmann, ed., RILEM, Aedificatio Publishers, Freiburg, Germany, 1997, pp. 435-456).

2. Bažant, Z.P.; Osman, E.; and Thonguthai, W., "Practical Formulation of Shrinkage and Creep in Concrete," *Materials and Structures* (RILEM, Paris), V. 9, 1976, pp. 395-406.

3. Bažant, Z.P., and Panula, L., "Practical Prediction of Time-Dependent Deformations of Concrete," *Materials and Structures*, V. 11 (1978), pp. 307-316, 317-328, 415-424, 424-434; V. 12 (1979), pp. 169-174.

4. Bažant, Z.P., "Criteria for Rational Prediction of Creep and Shrinkage of Concrete," *The Adam Neville Symposium: Creep and Shrinkage—Structural Design Effects*, SP-194, A. Al-Manaseer, ed., American Concrete Institute, Farmington Hills, MI, 2000, pp. 237-260.

5. Křístek, V., and Kohoutková, A., "Serviceability Limit State of Prestressed Concrete Bridges," *Proceedings of the 1st* fib *Congress 2002 Concrete Structures in the 21st Century*, Osaka, V. 2, Part 11, 2002, pp. 47-48.

6. Bažant, Z.P. "Theory of Creep and Shrinkage in Concrete Structures: A Précis of Recent Developments," *Mechanics Today*, S. Nemat-Nasser, ed., Pergamon Press, V. 2, 1975, pp. 1-93.

7. Bažant, Z.P., "Numerical Analysis of Creep of an Indeterminate Composite Beam," *Journal of Applied Mechanics*, Trans. ASME, Ser. E, V. 37, 1970, pp. 1161-1164.

8. Bažant, Z.P., and Najjar, L.J., "Comparison of Approximate Linear Methods for Concrete Creep," *Journal of the Structural Division*, ASCE, V. 99, No. ST9, 1973, pp. 1851-1874.

9. Ghali, A., and Elbadry, M., "Serviceability Design of Continuous Prestressed Concrete Structures," *PCI Journal*, V. 34, No. 1, Feb. 1989, pp. 54-91.

10. ACI Committee 209, "Prediction of Creep, Shrinkage, and Temperature Effects in Concrete Structures (ACI 209R-92) (Reapproved 1997)," American Concrete Institute, Farmington Hills, MI, 1992, 47 pp.

11. Bažant, Z.P., and Baweja, S., "Creep and Shrinkage Prediction Model for Analysis and Design of Concrete Structures—Model B3 (RILEM Recommendation)," *Materials and Structures*, V. 28, 1995, pp. 357-365 (with Errata, V. 29, Mar. 1996, p. 126).

12. Bažant, Z.P., and Baweja, S., "Creep and Shrinkage Prediction Model for Analysis and Design of Concrete Structures: Model B3," *The Adam Neville Symposium: Creep and Shrinkage—Structural Design Effects*, SP-194, A. Al-Manaseer, ed., American Concrete Institute, Farmington Hills, MI, 2000, pp. 1-83.

13. Křístek, V.; Petřík, V.; and Pilhofer, H.-W., "Creep and Shrinkage Prediction on the Web," *Concrete International*, V. 23, No. 1, Jan. 2001, pp. 38-39.

14. Vítek, J.L., "Long-Term Deflections of Large Prestressed Concrete Bridges," *CEB Bulletin d'Information No. 235–Serviceability Models–Behaviour and Modelling in Serviceability Limit States Including Repeated and Sustained Load*, CEB, Lousanne, 1997, pp. 215-227 and 245-265.

Received and reviewed under Institute publication policies.

Vladimír Křístek is Professor of Civil Engineering and Deputy Head of Department, Faculty of Civil Engineering, Czech Technical University, Prague, Czech Republic. He is Vice President of the Czech Society of Civil and Structural Engineers, founding member and chair of the Division of Civil and Structural Engineering of the Engineering Academy of Czech Republic, and an honorary member of the Czech Concrete Society. He is Partner of the design firm Křístek, Trčka, Ltd., in Prague.

Photo W.F. Pfeffer

Zdeněk P. Bažant, FACI, is McCormick Institute Professor and W.P. Murphy Professor of Civil Engineering and Materials Science at Northwestern University. He is a member of the National Academy of Sciences and National Academy of Engineering; foreign member of Austrian, Czech, and Italian academies; and a Registered Structural Engineer in Illinois. He has received six honorary doctorates (Prague, Karlsruhe, Boulder, Milan, Lyon, and Vienna) and many medals, including ASCE's Theodore von Karman medal. A member of several ACI technical committees, including ACI Committee 209, Creep and Shrinkage in Concrete, he previously chaired ACI Committee 446, Fracture Mechanics.

Miloš Zich received a PhD in the theory of structures and is a lecturer at the Faculty of Civil Engineering, Technical University of Brno, Czech Republic. He is a Chartered Engineer, Czech Chamber of Chartered Engineers, in the field of building construction and has published a number of papers in technical journals and conference proceedings.

Alena Kohoutková is Associate Professor of Civil Engineering and Head of Department, Faculty of Civil Engineering, Czech Technical University. She is a member of *fib* TG 4.1, head of several research teams, and a member of the Doctoral Examination Committee and the Czech Concrete Society. She has published more than 100 papers in technical journals and conference proceedings.

UNEQUALLED BY "OR EQUALS"

When you specify a Metzger/McGuire floor joint filler for your client's project, you're not just selecting a product...you're providing your client with the best floor joint protection system the industry has to offer.

Every Metzger/McGuire product comes packaged with our *Quality Assurance Program*. From a project's inception through its completion, we are continually committed to ensuring that any product we provide is of the highest quality and is installed under the best conditions the project will allow. Most importantly, we work at every level to ensure our products are installed by a qualified contractor and are installed properly, *as specified*, in order to best protect your client's floor.

Unequalled Commitment...Unequalled Protection

Does Your Client Deserve Anything Less?

METZGER/McGUIRE

Industry Standard Industrial Floor Joint Fillers & Repair Products

800-223-MM80

www.metzgermcguire.com

CIRCLE READER CARD #20